Applied Energy 211 (2018) 41–49

Contents lists available at ScienceDirect

Applied Energy

journal homepage: www.elsevier.com/locate/apenergy

Towards unsupervised learning of thermal comfort using infrared thermography

Ali Ghahramani[a], Guillermo Castro[a], Simin Ahmadi Karvigh[a], Burcin Becerik-Gerber[b,*]

[a] Sonny Astani Dept. of Civil and Environmental Engineering, Viterbi School of Engineering, Univ. of Southern California, KAP 217, 3620 South Vermont Ave., Los Angeles, CA 90089-2531, United States

[b] Sonny Astani Dept. of Civil and Environmental Engineering, Viterbi School of Engineering, Univ. of Southern California, KAP 224C, 3620 South Vermont Ave., Los Angeles, CA 90089-2531, United States

HIGHLIGHTS

- A non-contact and non-invasive data acquisition method via infrared thermography was utilized.
- A hidden Markov model learning approach is introduced to capture dynamic thermal comfort.
- Comfort is achieved via preventing existence of uncomfortable conditions as a logical inference.
- 82.8% of prediction accuracy for detection uncomfortable conditions was obtained.
- Generalizing hyper-parameters of the model enables unsupervised learning of thermal comfort.

ARTICLE INFO

Keywords:
Thermal comfort
Human sensing
Infrared thermography
Personal comfort
Unsupervised learning
Hidden Markov models

ABSTRACT

Maintaining thermal comfort in built environments is important for occupant health, well-being, and productivity, and also for efficient HVAC system operations. Most of the existing personal thermal comfort learning methods require occupants to provide feedback via a survey to label the monitored environmental or physiological conditions in order to train the prediction models. Accuracy of these models usually drops after the training process as personal thermal comfort is dynamic and changes over time due to climatic variations and/or acclimation. In this paper, we present a hidden Markov model (HMM) based learning method to capture personal thermal comfort using infrared thermography of the human face. We chose human face since its blood vessels has a higher density and it is not covered while performing regular activities in built environments. The learning algorithm has 3 hidden states (i.e., uncomfortably warm, comfortable, uncomfortably cool) and uses discretization for forming the observed states from the continuous infrared measurements. The approach can potentially be used for continuous monitoring of thermal comfort to capture the variations over time. We tested and validated the method in a four-day long experiment with 10 subjects and demonstrated an accuracy of 82.8% for predicting uncomfortable conditions.

1. Introduction

Buildings account for about 30% of the total energy consumption in the world [1] (50% of which is associated with HVAC systems) and substantially contribute to the climate change (i.e., 30% of the global greenhouse gas emissions [2]). Heating, Ventilation, and Air Conditioning (HVAC) systems, responsible for providing thermal comfort in buildings, often use time-invariant setpoints derived from thermal comfort standards, such as the ASHRAE Standard 55 [3]. In several cases, this reliance on time-invariant setpoints has caused HVAC systems not to perform as desired, causing inefficiencies [4,5]. More recent models (e.g., adaptive models) account for climate variations for estimating occupants' thermal sensations [6]. However, prior research demonstrated that existing thermal comfort models do not account for several influential static and dynamic factors [4]. Static factors (e.g., race, gender [7]) are time-invariant across individuals, while dynamic factors (e.g., acclimation, age, and food intake [8–12]) make thermal comfort dynamic over time [13]. Although the impact of static factors on thermal comfort might be quantifiable through extensive and exhaustive field experiments, it is not trivial to quantify and learn the impact of dynamic factors. Lack of real-time access to building occupants' thermal comfort prevents control strategies to select temperature

* Corresponding author.
E-mail addresses: aghahram@usc.edu (A. Ghahramani), guille13lg@gmail.com (G. Castro), ahmadika@usc.edu (S.A. Karvigh), becerik@usc.edu (B. Becerik-Gerber).

https://doi.org/10.1016/j.apenergy.2017.11.021
Received 20 July 2017; Received in revised form 10 October 2017; Accepted 2 November 2017
Available online 10 November 2017

setpoints, which are more energy efficient. Potential savings of using comfort-driven and energy-aware set points vary based on the building size, type, construction materials, and climate in the range of 4–32% [14,15].

The inability of existing thermal comfort models to accurately estimate dynamic personal thermal preferences has led the researchers to explore various real-time thermal comfort sensing methods that are feasible to be used in buildings. Thermal comfort is defined as the condition of mind that expresses satisfaction with a thermal environment [16]. Consequently, thermal comfort can be measured directly only by surveying individuals about their comfort. Existing research and industry efforts to capture personal thermal comfort requires occupants to continuously provide feedback via surveys (e.g., surveys delivered through web interfaces [17]). Survey based methods are aimed to directly collect thermal preferences of occupants and consequently require the individuals to continuously answer questionnaires about their thermal comfort levels. Due to the advancements in participatory sensing methods, occupants can provide thermal comfort feedback via a web interface or an app to make the surrounding thermal environment comfortable. Evidently, survey based models identify comfort levels more accurately than the environmental and physiological measurement based models as they try to directly extract the "state of mind" of a person, however, they require continuous and frequent user feedback. Since it is impractical to continuously query occupants for their states of comfort, researchers have focused on environmental measurement based methods that aim to use training labels to correlate thermal comfort states (through continuous occupancy feedback) with environmental measurements (e.g., indoor air temperature). However, sensor and occupant locations in a built environment, as well as the size/volume of an environment make the trained models difficult to generalize. Moreover, methods based on the measurements of environmental factors do not take into account time-dependent variations into consideration unless continuous occupant feedback is provided. A comprehensive review of the two group of methods can be found in our earlier publication [18].

To reduce or ultimately eliminate the need for continuous feedback requirements for training of personal comfort models, physiological responses (e.g., skin temperature, heart rate, core temperature [19,20]) could be used to learn comfort. Physiological measurement based approaches are built upon the principle that physiological responses can be correlated with thermal discomfort. In other words, comfort is potentially maintained if no uncomfortable conditions occur. Hence, correlating the monitored measurements with occupant feedback enables predictive models to estimate an occupant's probability of discomfort. For example, the authors of [21] introduced a data driven predictive method that integrates personalized factors with a generalized model of the body heat balance. The model coefficients were calculated dynamically based on comfort votes via minimizing an error function (i.e., least square) of coefficients. Since the data collection was done on a daily basis, the authors argued that the modeling account for time variations of comfort. In [22], a deep artificial neural network (ANN) learning technique was used for classifying environmental conditions into three categories: comfortable, uncomfortably warm, and uncomfortably cool. The ANN algorithm had 4 input layers (i.e., air temperature, radiant temperature, air flow, air humidity) and 5 hidden layers. The algorithm was trained with the comfort votes of the test subjects under controlled experiments. However, the time dependent variations of thermal comfort were not included in the study. The authors of [23] developed a heuristic based method, which relates occupants' thermal sensations with body exergy usage rate. Their results showed that both the radiative and convective heat exchanges between an environment and a human body are satisfactory measures of body exergy usage rate. Time dependent variations were assumed to be inherently integrated in the exergy.

An adaptive thermal comfort modeling technique, which used the PMV (predictive mean vote) model as a prior model, was introduced in [24]. The model calculated an adaptation coefficient, which decreased or increased the estimated PMV values. The adaptation coefficient was calculated based on a field study that took into account local climate, culture, and social backgrounds. In [25], the authors developed an adaptive fuzzy-logic based algorithm that learns comfort on-line, using individuals' actions on thermostats and environmental conditions. The fuzzy sets were aligned with the desired changes to the thermostat. A multiple regression model that takes mean skin temperature and its time differential as input and predicts transient thermal sensations was introduced in [20]. The results showed strong correlations (with 0.8 as correlation coefficient) for the proposed technique for predicting the sensations. The authors in [26] explored the applicability of using heart rate variability (HRV) index and the electroencephalograph (EEG) as an indicator of thermal comfort. They carried out experiments to investigate how environmental temperature influences the HRV and EEG of people and relate the two factors with the thermal comfort. They found that HRV index may be closely related to thermal comfort sensations. However, their EEG analysis demonstrated that although there could be a relationship between comfort and the measurements, future research is required to make use of the EEG measurements. In [27], authors presented a mathematical model of thermal sensation based on the neurophysiology of thermal reception. Experimental data from 12 subjects were used to develop the model and 8 subjects to validate it. The collected data included skin and core temperature measurements. For the development dataset, 12 young adult males were exposed to transient conditions where air temperature varied from 30 to 20 to 35 to 30 °C. For validation, 8 young adult males were exposed to relatively different transient conditions where air temperature varied from 17 to 25 to 17 °C. The predictive model had a mean r-squared error of 0.89 for the training stage and the relatively low mean r-squared error of 0.38.

The majority of the models mentioned above require the occupants to continuously provide feedback to train the predictive model. In other words, occupants are responsible for training the learning model to adapt to their thermal preferences. Thus, there is a need for a data collection technique that enables unsupervised personal thermal comfort learning techniques. Moreover, current physiological based methods require the sensing system to be directly connected or inserted into the human body. To be practical and adapted widely by building occupants, this modeling technique should be built using the data collected by a non-invasive sensing technique. Providing real-time personal thermal comfort information to HVAC controllers could enable designing new optimization and control paradigms that select more energy efficient setpoints while ensuring occupants' comfort.

One of the responses of human body to thermal stress (i.e., heat or cold) relates to cutaneous vessels. The sympathetic neural control of skin blood flow includes the noradrenergic vasoconstrictor system and cholinergic active vasodilator system [28,29]. Accordingly, thermoregulation system alters heat exchange with the environment by modifying the skin blood flow through cutaneous arterioles and veins [30]. Distribution of cutaneous vessels is not uniform across a human body. On areas around the human face, the density of vessels is considerably higher [30], enabling higher blood circulation. In addition, human face is usually not covered by clothing in buildings therefore infrared radiation on a human face could be monitored easily. Therefore, in this paper, we used facial skin temperature as a measure of skin blood flow to characterize the thermoregulation responses of human body to hot and cold stresses. We specifically focused on four points on face (i.e., ear, nose, front face, and cheekbone) as they are located on different cardiovascular territories [30] and behave differently under hot or cold thermal stimuli [31]. By monitoring the thermoregulation performance, we aim to identify the thermoneutral zone and consequently predict thermal comfort. There are several methods for measuring skin blood flow, including venous occlusion plethysmography, Doppler ultrasound, laser Doppler, thermostrom, photoelectric plethysmography, impedance and radioactive isotopes [32–34]. Even though these methods have shown promising results for monitoring skin blood flow,

they have drawbacks that prevent their applications for regular daily office activities comfort monitoring. These drawbacks include: (1) these devices are required to be attached to a human body, (2) users are required to avoid any movement as motion introduces large errors [35], (3) device should be set with a certain angle or position, and (4) the fact that limb fat content impact the results.

To address these challenges, in a previous study [31], we designed and tested a wearable device (i.e., an eyeglass with infrared sensors) to continuously monitor skin radiations on several points on human face to collect physiological data in a non-invasive way. In present study, we used the data collected by this device and developed a hidden Markov model (HMM) based learning method to reduce and ultimately eliminate the need for user thermal feedback. The HMM model has three hidden states (i.e., uncomfortably warm, comfortable, and uncomfortably cool) and an arbitrary number of observable states. We used the average temperature of monitored facial points as the observed variable in the hidden Markov model to minimize the bias in the calculation by using a single measurement. We also used a static transition probability matrix and a dynamic emission probability matrix by modeling 3 probability distributions based on the collected data. Since the hidden Markov models require discrete values for observed variables, we utilized a discretization method to create a vector of observed states. To test our learning method, we designed a four-day long experiment, which included hot and cold indoor environmental conditions, and collected physiological data using the wearable device and the comfort levels via a user interface (for ground truth). The paper is organized as follows. The proposed learning method, which includes the data-driven modeling processes for the hidden Markov model and the comfort state estimation process, is presented in Section 2. Section 3 provides the details of the data collection procedures. We present the results and the performance metrics in Section 4. Section 5 provides a discussion on generalization of results and potential real-world applications of the presented method. Section 6 discusses the limitations of the study and presents the future steps for research. Finally, Section 7 concludes the paper.

2. Methodology

To monitor human thermoregulation responses to thermal stimuli, we used a non-invasive method for indirectly determining skin blood flow by infrared thermography using infrared sensors. For our explorations, we designed/ran an experiment (see Section 3) in order to monitor thermoregulation performance during hot and cold stress while collecting subjective thermal comfort votes. Thermal comfort votes are the conscious perceptions of an individual to a thermal environment, whereas the thermoregulation system regulates the unconscious response of an individual to a thermal environment.

2.1. Comfort learning method

In order to learn the states of thermal comfort, we used a hidden Markov model (HMM) based learning method to estimate the hidden states based on the time-series of skin infrared radiations measured in temperature values. An HMM is a type of dynamic Bayesian network that aims to estimate the hidden states of an unobserved Markov chain via observing the variables that are dependent on the hidden Markov chain states. In other words, the observed variables are probabilistic functions of hidden states and are time-wise dependent (i.e., the Markovian behavior). In the case of thermal comfort modeling, we have three hidden states: (1) uncomfortably warm conditions, (2) comfortable conditions, and (3) uncomfortably cool conditions. The observable variable, which is the average skin temperature, is a continuous variable with different behaviors across occupants. Since the HMM requires the observable states to be discrete, we rounded the temperature values to the closest integer value. Fig. 1 demonstrates the probabilistic architecture of the HMM, used in comfort learning. There are 3 hidden states (i.e., x_1: uncomfortably warm, x_2: comfortable, and x_3: uncomfortably cool) but the are hidden, and the observed states (**y**) are discretized skin temperature measurements. **TP** is the transition probability matrix and each element demonstrates the probability that a hidden state (x_i) to remain in the same state or transit to another state. **EP** is the emission probability transition matrix. Each line of the matrix demonstrates the probability of a hidden state to result in different skin temperature values. Since the range of skin temperatures might be different from person to person, we represent the state as a vector (**y**) with a variable size.

Fig. 2 demonstrates the sequential behavior of the observed variables and the hidden sequence of the states. As it can be seen, the observed state is a probabilistic function of the hidden state and hidden state is the probabilistic function of the previous hidden state. In other words, comfort states are dependent on the previous comfort states and skin temperatures are the functions of comfort states. If skin temperatures change considerably over time in a sequential way, this represents a change in the hidden state of thermal comfort.

The Viterbi algorithm [36] is used on the HMMs to estimate the hidden state sequence with the maximum probability from the observed states. In our case, the hidden state sequence is the sequence of thermal comfort states that has the highest probability of occurrence based on the observed time-series of skin temperature. There are three inputs for formulating the Viterbi algorithm on the HMM (see Fig. 2): (1) transition probability matrix (TP), (2) emission probability matrix (EP), and (3) initial probabilities (π). The Viterbi algorithm uses a recursive structure (see Eqs. (1) and (2)) to find the highest probability hidden state sequence (see Eq. (3)). We provide details on how to calculate these unknown values in the following paragraphs.

Let $\delta_t(j)$ be the probability of the most likely path ending with x_j at time t.

$$\delta_t(x_j) = \max_{x_1,x_2,\ldots,x_{t-1}} P(X_1 = x_1, X_2 = x_2, \ldots, X_t = x_j) \quad (1)$$

Eq. (1) recursively relates to past observations:

$$\delta_t(j) = \max_i \delta_{t-1}(i) tp_{ij} EP(y_t | X_t = s_j) \quad (2)$$

The most like path at the point x_j is

$$\text{argmax}_j \delta_t(x_j) \quad (3)$$

When the recursive equation reaches the first state of the sequence, it calculates the most likely path based on the initial probabilities (tp_{ij} is replaced with π_i). Here, we do not provide details on the Viterbi algorithm efficiency mechanisms and procedures for calculating the highest probability path as it is a well-known approach. Details on the algorithm and code implementations can be found in [36,37].

Sample data or prior knowledge has to be provided to the abovementioned matrices for the Viterbi algorithm. Specifically, we use a heuristic based on the nature of thermal comfort to simplify the transition probability (TP) matrix development. The heuristic is: the probability of transitioning from a comfortable state to any of the uncomfortable states is smaller than remaining in the comfortable state, and vice versa ($tp_{ii} > 0.5$), due to the fact that thermal comfort is a relatively stable variable when it is studied per second (our measurement rate). In Section 4 and Fig. 8, we provide a sensitivity analysis on the performance of the algorithm and the transition to validate the heuristic. In addition, the probability of moving from an uncomfortably warm condition to an uncomfortably cool condition is zero as it has to transition through comfortable conditions ($tp_{13} = tp_{31} = 0$). Assuming a symmetrical transition matrix, and similar probabilities for transitioning from a comfortable state to uncomfortable states, we simplified the matrix to have one hyper parameter (tp). For the initial probability vector (π), we use the knowledge in our experiments that the initial condition starts in comfortable conditions and set all the probabilities of other conditions to zero. However, it should be noted that these values can be chosen differently based on the initial conditions or be set to

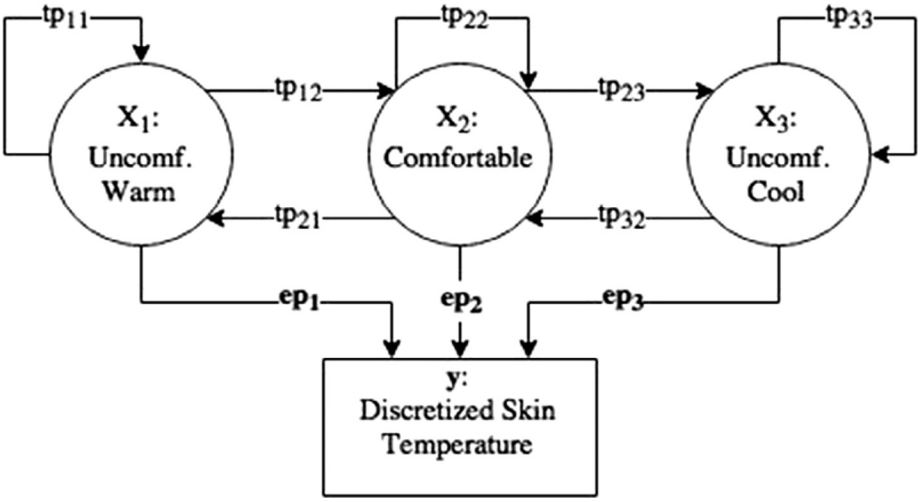

Fig. 1. Graphical representation of the hidden Markov model.

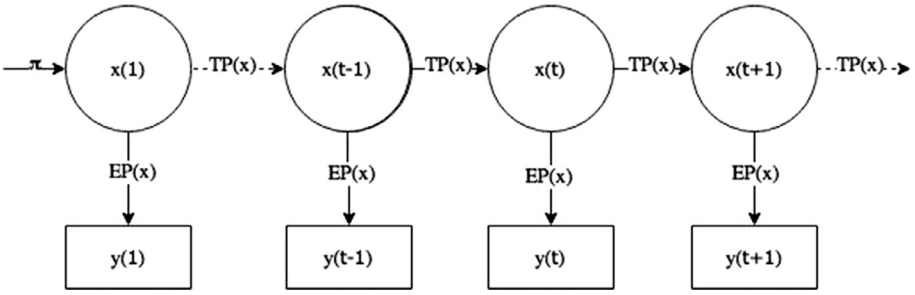

Fig. 2. Markovian behavior of the hidden states and conditional dependence of the observed variables.

similar values to represent unknown conditions. It should also be noted that although the hidden states transition probabilities are set to be fixed in the HMM formulation, this does not represent a fixed likelihood of change in the hidden thermal states. Recognizing a change occurs with accumulating enough evidence on the observable states' measurements and corresponds to a transition in the hidden states which are actual comfort states.

For the emission probability (EP) matrix, we use a probabilistic data driven method to compute the rows based on a similar heuristic used for the transition matrix. The heuristic is: the uncomfortably warm and cool states both have a half normal distribution (with different skews) for depicting the observed variables (i.e., temperature) in the range of measured observed variables. In other words, an uncomfortably warm state is more likely to result in skin temperatures close to the upper bound of measurements while the uncomfortably cool state is more likely to result in skin temperatures close to the lower bound of measurements. In addition, the comfortable state would follow a normal distribution for the observed temperatures. To simplify the computation of the probability distributions, we assume similar standard deviations for all of them, and set the value to the standard deviation of the whole data set of the observed temperature values. The starting point (the point with the highest probability for the half-normal distribution) for uncomfortably warm probability distribution is set to the lowest value observed in the temperature time-series. Similarly, the starting point for the uncomfortably cool state is set to the highest value observed in the temperature time-series.

In our evaluations, we focused on uncomfortable conditions because predicting and addressing the uncomfortable conditions is the main goal of a learning system in this context. By preventing the occurrence of the uncomfortable conditions via a control system, the learning system lays the foundation for the occupants to perceive comfort. Therefore, we assessed the performance of our proposed learning method based on the specificity measure $\left(\frac{TN}{TN+FP}\right)$ of the thermal comfort votes of all occupants. It should be noted that TN + FP is the total number of uncomfortable votes. In addition, FP (conditions labeled as comfortable which are not true) is the error, which should be minimized, while the FN (conditions labeled as uncomfortable but are actually comfortable) can be tolerated. FN is an acceptable error from the comfort perspective because when a condition is incorrectly labeled as uncomfortable, the occupant remains perceiving comfort as long as the FP error is minimized. However, in this case, the HVAC system might consume more energy trying to make an already comfortable occupant comfortable (labeled as uncomfortable).

2.2. Compliance with ASHRAE 55

ASHRAE Standard 55 (thermal environmental conditions for human occupancy) uses the PMV-PPD model to define the comfortable indoor thermal conditions [3]. Specifically, the standard requires the percentage of people dissatisfied (PPD) to be less than 20%, which implies that at least 80% of the occupants in a building should be thermally comfortable. If we define an indicator function (see Eq. (4)) for an occupant to be comfortable or not, and apply the probability threshold of 80% (P(X= 1) = 0.8), the expectation of the indicator function would be 0.8 (see Eq. (5)).

$$X=\begin{cases}1 & \text{if Occupacnt i is Comfortable}\\ 0 & \text{if Occupacnt i is Uncomfortable}\end{cases} \tag{4}$$

$$E(X) = P(X=1) = 0.8 \tag{5}$$

Consequently, the expectation of the indicator function for the population of building occupants (i.e., the expected percentage of satisfied occupants) would be 80% (see Eq. (6)). Thus, we would meet the ASHRAE standard requirements.

$$E\left(\sum_{i=1}^{n} X\right) = \sum_{i=1}^{n} (E(X)) = 0.8*N \tag{6}$$

In the cases, where the Viterbi algorithm's hidden state sequence maximum probability falls below 80%, the algorithm fails to find a range of environmental conditions that meet the standard's requirements. In such cases, we recommend to select the state with the highest probability of occurrence until the probability reaches 80%. However, since these uncertainties happen in the transition stages between the hidden states, other strategies can be selected, such as selecting the state which demonstrates a growth in the probability of occurrence.

3. Data collection

In order to validate our method, we collected physiological measurements and thermal comfort feedback of 10 test subjects (7 males and 3 females) in a shared office space in a university building in Los Angeles, California. According to the Köppen–Geiger climate classification [38], the climate of the city is classified as dry-summer subtropical. The duration of the experiment for each test subject was at least 2 h a day for four days: three days with the office thermostat set to provide comfortable conditions according to the subjects' preferences (three comfortable days) and one day deliberately with extreme temperature settings (an extreme day), so that the test subjects are exposed to different thermal stresses. The extreme day for all test subjects started from their comfortable condition (varies from person to person and we call it CC) and then were randomly exposed to CC to 29 °C to 18 °C (negative temperature gradient) or CC to 18 °C to 29 °C (positive temperature gradient). Our goal was to minimize the bias related to data collection in a specific day or a specific temperature setting. Each test subject was given an ID number and asked to communicate his/her votes with that ID number, using a user interface (Fig. 5) while wearing an eyeglass frame with four infrared sensors installed on an eye glass frame (Fig. 3). Fig. 4 illustrates the device worn by a male subject.

The sensors were fixed on the eyeglass frame to point to four facial points (i.e., nose, front face, back of ear, and cheekbone). Due to the differences in facial structures, the sensors pointed to an area as opposed to exact points for each test subject. However, our data collection results did not show any significant change in the measurements for different test subjects. We opted to use a fixed set of sensing points, rather than optimizing the locations of the sensing points since it requires a thermal camera to monitor every point simultaneously. The infrared sensor used to measure physiological responses were MLX90614, which is factory calibrated and has an accuracy of ± 0.1 °C with the resolution of 0.01 °C. The infrared sensor was tested in laboratories for human subjects research and recommended by the producer for medical applications [39]. Arduino UNO microcontrollers were used to collect the sensor measurements and store them into a database. The connections were all wired to insure a stable stream. The test subjects were able to move their head around while performing

Fig. 3. Eyeglass frame with four installed infrared sensors.

Fig. 4. A male subject wearing the infrared sensing system installed on an eyeglass frame.

regular office activities to replicate a real-world scenario. Through a real-time visualization of the sensor measurements, any issues with the data collection was identified and addressed immediately.

We used a thermal comfort scale (Fig. 5) to cover various thermal comfort levels [40]. For the data analysis, we grouped comfortably cool, comfortable, and comfortably warm votes as a single state (i.e., comfortable), and much too cool and uncomfortably cool votes as a single state (i.e., uncomfortably cool), and uncomfortably warm and much too warm votes as a single state (i.e., uncomfortably warm). The test subjects were required to provide thermal comfort votes (10 votes per day with a 15-min gap between the votes) during regular office activities (e.g., working with a laptop or computer). The votes provided by the participants were used as the ground truth. The heating sources were two electrical heaters and the cooling source was cooled air from a central air conditioning system controlled via a thermostat in the room. The test subjects were seated in a manner that they were not exposed directly to heat or cold. The temperature sensor used to monitor external heat stimuli was Aosong AM2302, which is calibrated with an accuracy of ± 0.5 °C and a resolution of 0.1 °C. Four sensors were placed around test subjects.

4. Results

Figs. 6 and 7 demonstrate the collected physiological and environmental measurements (cheekbone, ear, front face, nose, the average facial points, and room temperatures) from two test subjects.

There is a high correlation between the facial temperature measurements and thermal stimuli (i.e., room temperatures). However, the behaviors of single measurements are different, especially, during the extreme days. As explained earlier, although the room temperature is the only external stimulus, internal heat equilibrium and thermoregulation performance highly impact skin temperatures. Thus, even though environmental temperature is a highly influential factor, there are other factors important to thermoregulation performance and thermal comfort, impacting skin temperatures.

The data, collected from 10 test subjects, included 457 votes, of which 87 votes were uncomfortable and 370 votes were comfortable. Out of the 87 uncomfortable votes, 26 votes were uncomfortably cool and 61 votes were uncomfortably warm. As explained in Section2 2, we used the heuristics to reduce the complexity of the transition and emission probability matrices. The transition probability matrix has one hyper parameter (tp) that demonstrates the rate of transitions from the comfortable state to uncomfortable states and vice versa. The emission probability matrix has two half-normal and one normal distributions that are driven based on the data collected during the experiment and assumed to include all comfortable and uncomfortable conditions. Fig. 8 demonstrates the specificity measure of the algorithm and the ratio of the comfortable conditions states over all states as a function of the transition probability (tp) for all of the test subjects.

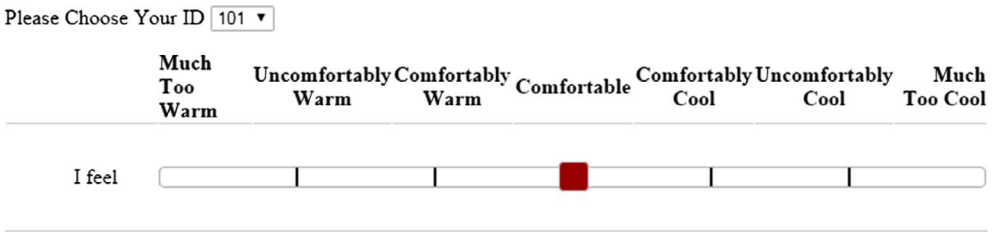

Fig. 5. User interface for collecting personal thermal comfort votes.

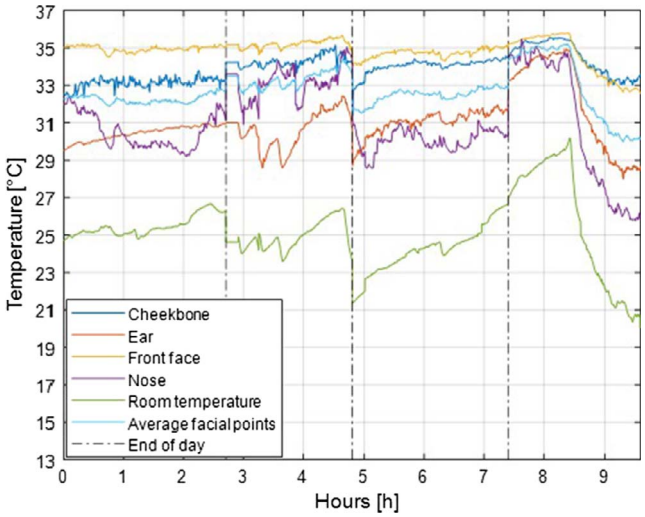

Fig. 6. Facial points and room temperature measurements for subject 1.

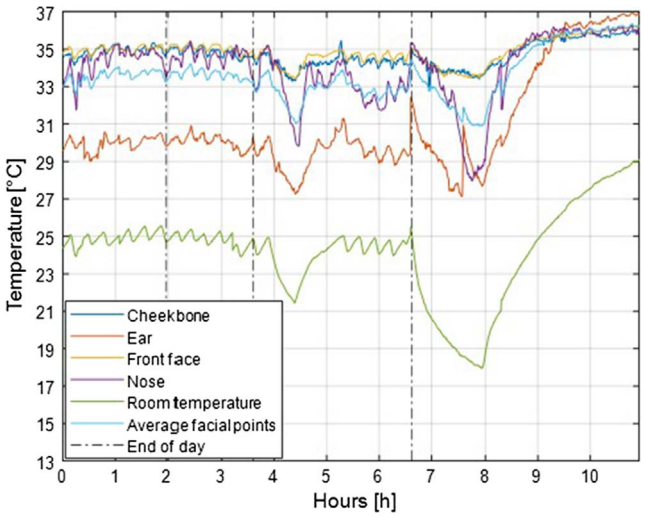

Fig. 7. Facial points and room temperature measurements for subject 2.

As it can be seen in Fig. 8, a smaller transition probability results in higher prediction performance (83%) while the ratio of the comfortable states holds relatively small values (49%). On the other hand, a higher transition probability results in lower prediction performance (46%) and higher ratio of comfortable states (76%). Accordingly, improving the performance of discomfort prediction would label many instances as uncomfortable, and therefore, the ratio of comfortable states decreases. It is interesting to note that the smaller tp ratio relates to a higher prediction performance of discomfort conditions. This is related to the sampling rate (1 measurement per second) and the fact that a smaller ratio better fits the measurement rates. The figure demonstrates the trade-off between the performance of comfort prediction and the ratio of comfortable conditions. In other words, an HVAC system might consume more energy to keep the comfortable states since the higher the focus on preventing uncomfortable conditions, the higher the constrains on the HVAC operations (a smaller ratio of comfortable environmental conditions).

Fig. 9 shows the precision $\left(\frac{TP}{TP+FP}\right)$ and recall $\left(\frac{TP}{TP+FN}\right)$ measures for different values of tp. As it can be seen, there is a trade-off between the precision and recall measures. The higher the precision (the accuracy of the algorithm for classifying comfortable conditions versus uncomfortable conditions), the lower the recall rate (the rate of the comfortable conditions detection). The starting point of the curve is associated with the lowest tp value. The figure demonstrates that reducing the FP and FN error cannot be realized simultaneously, implying that the improvement in uncomfortable conditions error (FP) has a negative impact on the comfortable conditions error (FN). The cost of FN (predicting a person is uncomfortable, but actually is comfortable) is less of an issue from the comfort perspective, because, in these kinds of scenarios, a likely change in the thermal environment does not necessarily make the person uncomfortable (i.e., comfortable conditions in this context is a subset of real comfort conditions). It is due to the fact that the HMM uses a continuous internal representation of comfort states and by classifying the states that the likelihood of discomfort is high as uncomfortable, the opposite condition (comfort) occurs. Therefore, if a control policy uses the results of the proposed method to change a condition in the environment, the change in the environmental conditions is intended to keep the observable states (physiological measurements) in a neighborhood that is very likely representing the hidden comfort state (heating in case the body is losing heat or cooling in case the body is accumulating heat).

Based on Fig. 8, we searched for better tp in smaller values (0.0000001, 0.000001, 0.00001, 0.0001, 0.001, 0.01). The specificity measure for all tested values was 82.8% and the ratio of comfortable conditions only changed very slightly. Therefore, any positive (non-zero) value between 0 and 0.01 can be set as the tp measure. In this study, we chose the transition rate of 0.01 for the development of the transition probability matrix. Applying the Viterbi algorithm to find the hidden state sequence with the maximum probability based on the emission and transition probability matrices results in finding the probability of all comfort states at each temperature point, and consequently, the most likely comfort state path. Figs. 10 and 11 demonstrate the probability of all hidden states and the Viterbi path (highest probability path) over the course of the temperature time-series for test subjects 1 and 2. The thermal votes of the test subjects are also presented in the figures.

As it can be seen in Figs. 10 and 11, the HMM was able to provide a probability greater than 80% for the prediction of the most data points that satisfy the requirements for compliance with thermal comfort standards. The immediate transitions (vertical green, blue and red lines) is due to the small transition probability (tp) which is hyperparameter optimized for the optimal performance of the algorithm. Larger tp would make the lines having lower slopes, and would have resulted in a lower comfort prediction accuracy. The Viterbi path (the path with the highest probability) demonstrates a value close to 1 for the majority of the cases due to high rate of sensor measurements with respect to the transition probability. The HMM also captured the thermal comfort states on majority of the cases (the color of the dashed lines matches the color of the solid lines in the region with probability

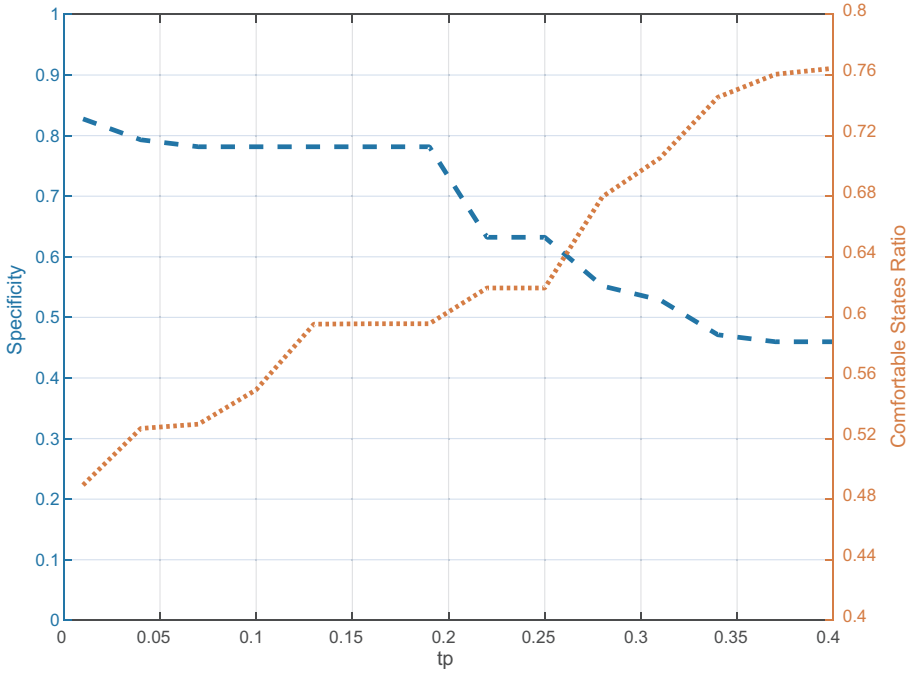

Fig. 8. Specificity $\left(\frac{TN}{TN+FP}\right)$ measure of the algorithm and the ratio of the comfortable states for all of the test subjects.

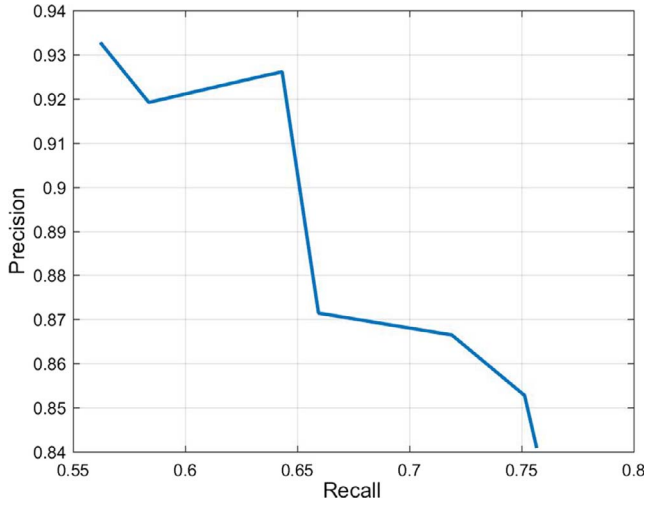

Fig. 9. Precision and recall curve for all of the test subjects.

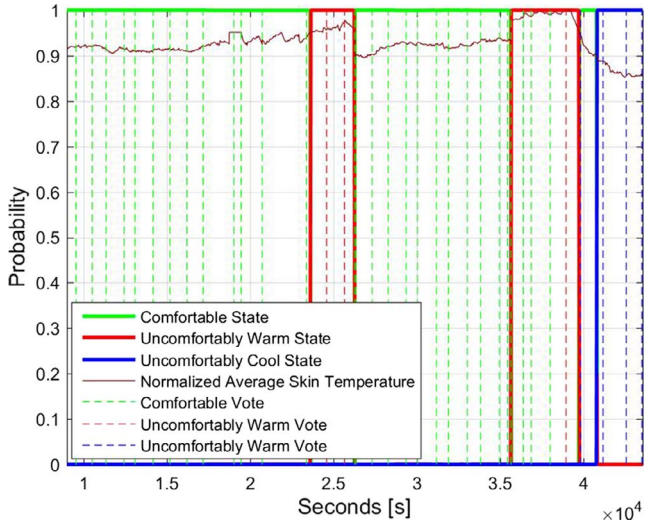

Fig. 10. Hidden states probabilities and comfort votes for subject 1.

1).

Overall, the average accuracy for predicting uncomfortable votes (specificity measure) for all of the test subjects was 82.8%, which suggests that the proposed HMM based learning algorithm is capable of predicting thermal comfort without any need for occupant feedback. The accuracy for the uncomfortably warm conditions was 80.8% with a standard deviation of 15.5% across all test subjects and the accuracy for the uncomfortably cool conditions was 83.6% with a standard deviation of 20.8% across all test subjects, which demonstrates no considerable difference. Our proposed method addresses the requirement of detecting time dependent variations in the personal thermal comfort by continuously monitoring thermal responses of human body and not the subjective thermal votes from the occupants. The fact that this method removes the need for occupants to train a learning system indirectly addresses the problem of detecting time dependent variations in thermal comfort.

5. Discussion

Real-time facial skin blood flow monitoring enabled us to study thermal comfort under different thermal stimuli in an office environment. The thermal comfort learning method, introduced in this paper, uses a HMM structure to estimate the hidden states of comfort and we demonstrated its performance by tuning the HMM internal hyper parameters. Since the optimal hyper parameters were similar among subjects and follow a logical reasoning, we envision a more comprehensive study of personal thermal comfort (with more test subjects) would provide more generalizations for the model and lead to unsupervised learning of personal thermal comfort. We also argue that by focusing on the capturing uncomfortable conditions and preventing them, logic asserts that we could achieve comfortable conditions. The proposed method can be integrated to these control policies and can enhance them by providing online data about personal thermal comfort requirements. However, more research is required to understand how control paradigms based on presentation of uncomfortable states can be

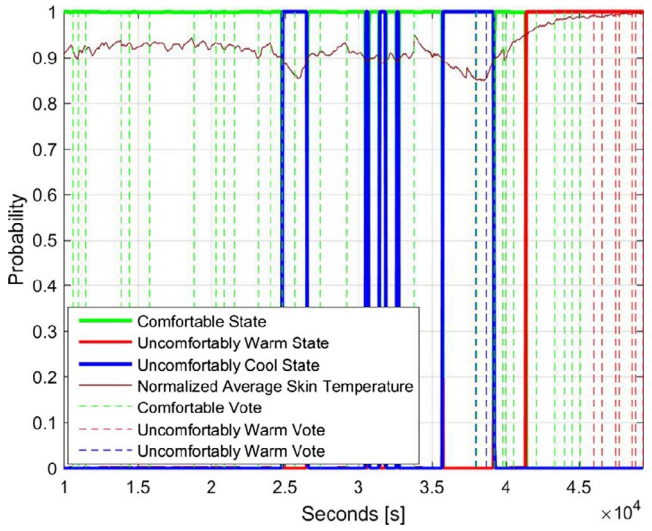

Fig. 11. Hidden states probabilities and comfort votes for subject 2.

optimized as any control action may have either negative or positive energy consumption consequences, depending on the building, climate, and other influential characteristics [14,41–45]. We demonstrated that there is a trade-off between the accuracy for detecting uncomfortable conditions and the overall ratio of comfortable conditions. This implies that more constraints would be imposed on an HVAC system when preventing uncomfortable conditions. In addition, the precision and recall trade-off analysis demonstrated that the FP and FN error reduction cannot be realized simultaneously, implying that improvements in the error of detection of uncomfortable conditions have a negative impact on the error of detecting comfortable conditions. Energy savings from optimally selecting HVAC temperatures in office buildings can be as high as 37% [14,15], although the savings differ based on the climate, building materials, and size. In addition, occupant behavior and utilization of new technologies in buildings might effect energy savings [45–48]. It is worth mentioning that the trade-off between the complexity of sensing devices/controllers and energy savings can play an important role for user adaption of these methods [46,49–54], which requires further investigations.

Perceived thermal comfort and control over the thermal environment have profound impacts on the office work performance and it can be used to boost workplace productivity [55]. In cases where skin blood flow can be used as a measure of physiological response to external stimuli, the proposed method can also be applied. For example, indoor or outdoor physical activities in forms of exercise result in a non-thermoregulatory change for cutaneous vasoconstriction as well as a thermoregulatory change for cutaneous vasodilation. Therefore, an initial vasoconstriction followed by a vasodilation is observed and can be monitored via the proposed sensing technique. Another use of the proposed sensing technique is for monitoring stress in indoor environments.

Acute psychosocial stress exposure decreases intestinal temperature and results in changes in skin temperature that follows a gradient-like pattern, with decreases at distal skin locations such as the fingertip and finger base and unchanged skin temperature at proximal regions such as the infraclavicular area [56]. Accordingly, our proposed method can be used to detect such acute stress by monitoring skin temperature variations.

6. Limitations and future work

The test subjects in our experiments were in healthy conditions and were asked to perform regular office activities while wearing the eyeglass frames equipped with infrared sensors. As stated previously, thermoregulation system is not the only driving factor that impact the skin blood flow and skin temperature. Accordingly, the effects of other factors on the physiological measurements, such as the activity intensity were not monitored and thus not considered in this study. In addition, in order to generalize the results, more human subject data are needed. Furthermore, the experiments were carried out between July 2015 and October 2015 and in one climate type. In the local climatic conditions, the outdoor temperatures were warm to hot. Therefore, the impact of weather variations in one climate or variations in multiple climates were not integrated in the analysis. However, we should emphasize on the fact that our method focuses on an individual's skin blood flow to study thermal comfort. This fact reduces the impact of other factors, which are considered static (i.e., clothing conditions, food intake).

The HMM formulation described in this paper uses the transition and emission probability matrices that were developed based on the heuristics and data driven techniques to reduce the complexity of the learning algorithm. However, both the emission and transition probability matrices can be developed and tuned via more advanced learning, which will be explored in a future research study. In addition, we used a numerical method for discretizing the temperature measurements. More advanced discretization methods can be used to improve the accuracy of the algorithm, which also be explored. We used the average skin temperature of several facial points for developing the learning algorithm. However, HMMs allow for multiple observable variables for learning purposes, which would likely improve the accuracy of the comfort prediction. We leave this topic for a future study. It should be noted that developing a comfortable and practical sensing device was not in the scope of this study. The proposed device and comfort learning method could be further developed for commercialization and potentially become available for public use. As a part of our future research, we plan to explore the optimal positions, distance factors, and sensing coverage of the infrared sensors.

7. Conclusions

Real-time access to an individual's personal thermal comfort allows HVAC system controllers to optimize energy consumption while ensuring thermal comfort and other indoor air quality requirements are satisfied. In this study, we introduced a non-invasive data acquisition method that used infrared thermography to provide real-time information about occupants' thermal comfort. We used a HMM based learning method to estimate hidden states based on the time-series of skin infrared radiations measured in temperature values. We sensed blood flow indirectly on human face, which has a high density of skin blood vessels and is often not covered by clothing. The HMM based learning algorithm has 3 hidden states (i.e., uncomfortably warm, comfortable, uncomfortably cool) and uses a discretization module for forming the observed states from the continuous infrared measurements. Unlike other models, our method requires no continuous user input or user interaction. In addition, we demonstrated how the personal thermal comfort learning method, introduced in this paper, is in compliance with thermal comfort standards' requirements. We tested the proposed method via four-day long controlled experiments with 10 subjects. Based on the 457 votes (87 uncomfortable votes and 370 comfortable votes), the proposed learning algorithm demonstrated an accuracy of 82.8% for predicting uncomfortable conditions with the precision measure of 93.3% and the recall measure of 56.22%. Specifically, the accuracy of for uncomfortably warm conditions was 80.8% and the accuracy for the uncomfortably cool condition was 83.6%. The proposed thermal comfort learning method can enhance the control process of HVAC systems by providing online data on occupants' thermal comfort requirements.

Acknowledgments

This material is based upon work supported by the U.S. National Science Foundation under Grant No. 1351701. Any opinions, findings, and conclusions expressed in this material are those of the authors and do not necessarily reflect the views of the National Science Foundation. Special thanks to all the participants and specifically to Xinran Yu for her contributions inn running the experiments.

References

[1] Doman LE, Arora V, Metelitsa A, Leahy M, Barden J, Ford M, et al. International Energy Outlook 2013, IEO2013 Report; July 2013.
[2] C. Initiative, Buildings and Climate Change; 2009.
[3] ASHRAE Standard, Standard 55-2004, Thermal environmental conditions for human occupancy; 2004.
[4] Van Hoof J. Forty years of Fanger's model of thermal comfort: comfort for all? Indoor Air 2008;18:182–201.
[5] Sekhar S. Thermal comfort in air-conditioned buildings in hot and humid climates–why are we not getting it right? Indoor Air 2016;26:138–52.
[6] Olesen BW. International standards for the indoor environment. Indoor Air 2004;14:18–26.
[7] Karjalainen S. Thermal comfort and gender: a literature review. Indoor Air 2012;22:96–109.
[8] Ning H, Wang Z, Ji Y. Thermal history and adaptation: does a long-term indoor thermal exposure impact human thermal adaptability? Appl Energy 2016;183:22–30.
[9] Uğursal A, Culp CH. The effect of temperature, metabolic rate and dynamic localized airflow on thermal comfort. Appl Energy 2013;111:64–73.
[10] Brager GS, de Dear RJ. Thermal adaptation in the built environment: a literature review. Energy Build 1998;27:83–96.
[11] Jendritzky G, de Dear R. Adaptation and thermal environment. Biometeorology for adaptation to climate variability and change. Springer; 2009. p. 9–32.
[12] Schellen L, van Marken Lichtenbelt W, Loomans M, Toftum J, De Wit M. Differences between young adults and elderly in thermal comfort, productivity, and thermal physiology in response to a moderate temperature drift and a steady-state condition. Indoor Air 2010;20:273–83.
[13] Ghahramani A, Tang C, Yang Z, Becerik-Gerber B. A study of time-dependent variations in personal thermal comfort via a dynamic bayesian network. In: Sustainable human–building ecosystems. p. 99–107.
[14] Ghahramani A, Zhang K, Dutta K, Yang Z, Becerik-Gerber B. Energy savings from temperature setpoints and deadband: quantifying the influence of building and system properties on savings. Appl Energy 2016;165:930–42.
[15] Ghahramani A, Dutta K, Yang Z, Ozcelik G, Becerik-Gerber B. Quantifying the influence of temperature setpoints. Build Syst Features Energy Consum 2015:1000–11.
[16] Ashrae AS. Standard 90.1-2004, Energy standard for buildings except low rise residential buildings. American Society of Heating, Refrigerating and Air-Conditioning Engineers, Inc; 2004.
[17] Zagreus L, Huizenga C, Arens E, Lehrer D. Listening to the occupants: a Web-based indoor environmental quality survey. Indoor Air 2004;14:65–74.
[18] Ghahramani A, Tang C, Becerik-Gerber B. An online learning approach for quantifying personalized thermal comfort via adaptive stochastic modeling. Build Environ 2015;92:86–96.
[19] Huizenga C, Zhang H, Arens E, Wang D. Skin and core temperature response to partial-and whole-body heating and cooling. J Therm Biol 2004;29:549–58.
[20] Takada S, Matsumoto S, Matsushita T. Prediction of whole-body thermal sensation in the non-steady state based on skin temperature. Build Environ 2013;68:123–33.
[21] Zhao Q, Zhao Y, Wang F, Wang J, Jiang Y, Zhang F. A data-driven method to describe the personalized dynamic thermal comfort in ordinary office environment: from model to application. Build Environ 2014;72:309–18.
[22] Liu W, Lian Z, Zhao B. A neural network evaluation model for individual thermal comfort. Energy Build 2007;39:1115–22.
[23] Simone A, Kolarik J, Iwamatsu T, Asada H, Dovjak M, Schellen L, et al. A relation between calculated human body exergy consumption rate and subjectively assessed thermal sensation. Energy Build 2011;43:1–9.
[24] Yao R, Li B, Liu J. A theoretical adaptive model of thermal comfort–adaptive predicted mean vote (aPMV). Build Environ 2009;44:2089–96.
[25] Bermejo P, Redondo L, Ossa DL, Rodriguez D, Flores J, Urea C, et al. Design and simulation of a thermal comfort adaptive system based on fuzzy logic and on-line learning. Energy Build 2012;49:367–79.
[26] Yao Y, Lian Z, Liu W, Jiang C, Liu Y, Lu H. Heart rate variation and electroencephalograph–the potential physiological factors for thermal comfort study. Indoor Air 2009;19:93–101.
[27] Kingma B, Schellen L, Frijns A, van Marken Lichtenbelt W. Thermal sensation: a mathematical model based on neurophysiology. Indoor Air 2012;22:253–62.
[28] Charkoudian N. Skin blood flow in adult human thermoregulation: how it works, when it does not, and why. 2003; 78: 603–12.
[29] Ishikawa J, Oshima M, Iwasaki F, Suzuki R, Park J, Nakao K, et al. Hypothermic temperature effects on organ survival and restoration. Sci Rep 2015;5.
[30] Taylor GI. The blood supply of the skin, Grabb and Smith's Plastic Surgery. 5th ed. Philadelphia: Lippincott-Raven; 1997. 47–59.
[31] Ghahramani A, Castro G, Becerik-Gerber B, Yu X. Infrared thermography of human face for monitoring thermoregulation performance and estimating personal thermal comfort. Build Environ 2016;109:1–11.
[32] Petrofsky JS. Resting blood flow in the skin: does it exist, and what is the influence of temperature, aging, and diabetes? J Diabetes Sci Technol 2012;6:674–85.
[33] Tripathi SR, Miyata E, Ishai PB, Kawase K. Morphology of human sweat ducts observed by optical coherence tomography and their frequency of resonance in the terahertz frequency region. Sci Rep 2015;5.
[34] Swain ID, Grant LJ. Methods of measuring skin blood flow. Phys Med Biol 1989;34:151–75.
[35] Chen Y, Lu B, Chen Y, Feng X. Breathable and stretchable temperature sensors inspired by skin. Sci Rep 2015;5.
[36] Viterbi AJ. Error bounds for convolutional codes and an asymptotically optimum decoding algorithm. Inf Theory, IEEE Trans 1967;13:260–9.
[37] Murphy KP. Machine learning: a probabilistic perspective. MIT Press; 2012.
[38] Peel MC, Finlayson BL, McMahon TA. Updated world map of the Köppen-Geiger climate classification. Hydrol Earth Syst Sci Discuss 2007;4:439–73.
[39] Sheet MD. MLX90614 family, single and dual zone infrared thermometer in TO-39; 2009.
[40] García JAO. A review of general and local thermal comfort models for controlling indoor ambiences, air quality. Rijeka: InTech; 2010.
[41] Barbeito I, Zaragoza S, Tarrío-Saavedra J, Naya S. Assessing thermal comfort and energy efficiency in buildings by statistical quality control for autocorrelated data. Appl Energy 2017;190:1–17.
[42] Chowdhury AA, Rasul M, Khan MMK. Thermal-comfort analysis and simulation for various low-energy cooling-technologies applied to an office building in a subtropical climate. Appl Energy 2008;85:449–62.
[43] Al-Sanea SA, Zedan M. Optimized monthly-fixed thermostat-setting scheme for maximum energy-savings and thermal comfort in air-conditioned spaces. Appl Energy 2008;85:326–46.
[44] Dounis A, Manolakis D. Design of a fuzzy system for living space thermal-comfort regulation. Appl Energy 2001;69:119–44.
[45] Mostavi E, Asadi S, Boussaa D. Development of a new methodology to optimize building life cycle cost, environmental impacts, and occupant satisfaction. Energy 2017;121:606–15.
[46] Rafsanjani HN, Ahn C. Linking building energy-load variations with occupants' energy-use behaviors in commercial buildings: non-intrusive occupant load monitoring (NIOLM). Proc Eng 2016;145:532–9.
[47] Ghahramani A, Karvigh SA, Becerik-Gerber B. HVAC system energy optimization using an adaptive hybrid metaheuristic. Energy Build 2017;152:149–61.
[48] Ghahramani A, Jazizadeh F, Becerik-Gerber B. A knowledge based approach for selecting energy-aware and comfort-driven HVAC temperature set points. Energy Build 2014;85:536–48.
[49] Rafsanjani HN, Ahn CR, Alahmad M. A review of approaches for sensing understanding, and improving occupancy-related energy-use behaviors in commercial buildings. Energies 2015;8:10996–1029.
[50] Rafsanjani HN, Ahn CR, Alahmad M. Development of non-intrusive occupant load monitoring (NIOLM) in commercial buildings: assessing occupants' energy-use behavior at entry and departure events. In: Sustainable human–building ecosystems; 2015. p. 44–53.
[51] Ahmadi-Karvigh S, Becerik-Gerber B, Soibelman L. A framework for allocating personalized appliance-level disaggregated electricity consumption to daily activities. Energy Build 2016;111:337–50.
[52] Chassin DP, Stoustrup J, Agathoklis P, Djilali N. A new thermostat for real-time price demand response: cost, comfort and energy impacts of discrete-time control without deadband. Appl Energy 2015;155:816–25.
[53] Xu X, Culligan PJ, Taylor JE. Energy saving alignment strategy: achieving energy efficiency in urban buildings by matching occupant temperature preferences with a building's indoor thermal environment. Appl Energy 2014;123:209–19.
[54] Ahmadi-Karvigh S, Ghahramani A, Becerik-Gerber B, Soibelman L. One size does not fit all: understanding user preferences for building automation systems. Energy Build 2017;145:163–73.
[55] Bluyssen PM. Towards new methods and ways to create healthy and comfortable buildings. Build Environ 2010;45:808–18.
[56] Vinkers CH, Penning R, Hellhammer J, Verster JC, Klaessens JH, Olivier B, et al. The effect of stress on core and peripheral body temperature in humans. Stress 2013;16:520–30.